DOI: 10.1002/chem.201101828

A 5′-Cap for DNA Probes Binding RNA Target Strands

Simone Egetenmeyer and Clemens Richert*[a]

Abstract: Detecting short RNA strands with high fidelity at any of the bases of their sequence, including the termini, can be challenging, since fraying, wobbling, and refolding all compete with canonical base pairing. We performed a search for 5′-substituents of oligodeoxynucleotides that increase base pairing fidelity at the terminus of duplexes with RNA target strands. From a total of over 70 caps, differing in stacking moiety and linker, a phosphodiester-linked sequence of the residues of L-prolinol, glycine, and oxolinic acid, dubbed **ogOA**, was identified as a 5′-cap that stabilizes any of the four canonical base pairs, with ΔT_m values of up to +13.1 °C for an octamer. At the same time, the cap increases discrimination against any of the 12 possible terminal mismatches, including mismatches that are more stable than their perfectly matched counterparts in the control duplex, such as A:A. A probe with the cap also showed increased selectivity in the detection of two closely related microRNAs, let7c and let7a, with a ΔT_m value of 9.2 °C. Melting curves also yielded thermodynamic data that shed light on the uniformity of molecular recognition in the sequence space of DNA:DNA and DNA:RNA duplexes. Hybridization probes with fidelity-enhancing caps should find applications in the individual and parallel detection of biologically active RNA species.

Keywords: DNA · hybridization probe · molecular caps · molecular recognition · RNA · RNA recognition

Introduction

Of the two canonical nucleic acids, RNA is more abundant in the cell, shows greater diversity in its functions, and has a greater propensity to fold into complex three-dimensional structures.[1] Whereas the sole role of DNA is to store genetic information, ribonucleotides have a host of roles, including forming the core components of the translational machinery, acting as the recognition motif in cofactors, and regulating gene expression through riboswitches[2] or microRNAs.[3–6] Understanding the biological roles of RNAs requires analytical methods for detecting them selectively, often against a genomic background. Highly selective detection is particularly important for short RNAs with roles in the regulation of gene expression, such as microRNAs, for which accuracy in the detection can be critical for medical diagnostics. Being short, many microRNAs do not lend themselves to routine amplification through reverse transcription and the polymerase chain reaction (PCR),[7] so that high fidelity hybridization is critical. Due to the abundance of closely related isoforms, high sequence selectivity is required at any given position of the duplex. Accurate hybridization is also required for many modern methods of massively parallel or ultrasensitive detection.[8] Molecular recognition through hybridization is challenging when the target has a high propensity to fold and to form alternative base pairs, such as G:U or U:G wobble base pairs, and when the sequence differences are in terminal regions, where fraying and wobbling is common.

Hybridization probes for the detection of RNAs are most frequently oligodeoxynucleotides, as DNA is less expensive to synthesize than RNA. Oligodeoxynucleotides are also chemically and enzymatically more stable than oligoribonucleotides. So, the most relevant type of probes for the detection of microRNAs are DNA strands that form DNA:RNA hybrid duplexes upon recognizing their target. If the level of affinity and selectivity required is not met by unmodified DNA, modified oligodeoxynucleotide probes are called for. Increasing target affinity and selectivity beyond that of natural DNA may be achieved with different approaches. The modifications may involve the backbone of the probe, as in locked nucleic acids (LNAs),[9] peptide nucleic acids (PNAs),[10] phosphoramidates,[11] or oligonucleotides containing 2′-fluoronucleosides.[12] Alternatively, the nucleobases may be modified[13,14] or substituents that aid the interrogation of the target structure may be introduced in the interior of the probes. Substituents may also be introduced at the termini of oligonucleotides.[15,16] 'Highly decorated' hybridization probes use a combination of 5′- and 3′-caps, as well as substituents in the interior of the sequence.[17] Such probes were introduced to aid the massively parallel detection of diverse DNA target sequences on microarrays by smoothing out the differences in duplex stability between

[a] Dipl. Chem. S. Egetenmeyer, Prof. C. Richert
Institut für Organische Chemie
Universität Stuttgart, 70569 Stuttgart (Germany)
Fax: (+49) 711-685-64321
E-mail: lehrstuhl-2@oc.uni-stuttgart.de

Supporting information for this article is available on the WWW under http://dx.doi.org/10.1002/chem.201101828.

duplexes with different G/C content[18] and ensuring high base pairing fidelity up to the very termini. It is desirable to also realize the potential of highly decorated probes for RNA detection.

Only a modest number of covalently attached ligands or 'caps' are known that increase target selectivity at the terminus of duplexes between probes and target strands.[19] We recently reported a cap for the 3′-terminus of DNA hybridization probes for binding RNA target strands,[20] as well as a number of caps for the 5′-terminus of probes binding DNA target strands.[16] However, no cap for the 5′-terminus of hybridization probes that increases fidelity in the recognition of RNA targets had been identified. Caps commercialized for the 5′-terminus of DNA probes binding DNA targets[19e,21] did not perform well when binding RNA target strands (see below). As a consequence, we initiated a search for 5′-caps on oligodeoxynucleotides that bind RNA targets. Here, we present the results of this search, together with data on the thermodynamics of duplex formation and base pairing fidelity at the terminus.

Results

Effect of the backbone on pairing selectivity at the terminus: Earlier work on molecular caps for the termini of hybridization probes has shown that the duplex-stabilizing effect depends on the backbone structure of the target strand.[19b] At first glance, this may seem surprising, as the base pairs formed are identical (G:C) or near-identical (A:T versus A:U) for DNA:DNA and DNA:RNA duplexes. If the caps were interacting predominantly with the nucleobases of the terminal base pair,[22] little selectivity should result. So, either the caps were strongly interacting with the backbone or were further enhancing an intrinsically lower stability and selectivity of base pairing at the termini of DNA:RNA duplexes.

To shed light on this issue for our present case of DNA:RNA duplexes, we first measured the melting points of octamer duplexes with all of the 16 possible combinations of nucleobases at the 5′-terminus. For this, we used the DNA probe *d*(**X**GGTTGAC), in which **X** is A, C, G, or T, and DNA or RNA target strands *d*(GTCAACC**Y**) or *r*(GUCAACC**Y**), in which **Y** at the 3′-terminus is A, C, G, T, or U. Figure 1 shows the drops in melting point induced by mismatches at the terminus for either type of duplex. The individual absolute T_m values can be found in Tables S1 and S2 in the Supporting Information. For seven out of twelve cases, the mismatch discrimination was found to be poorer for RNA compared with DNA as the target. The difference was particularly pronounced for the problematic cases, such as those with A at the 5′-terminus of the probe, for which non-Watson–Crick combinations A:A and A:G result in more stable mismatched DNA:RNA duplexes than the fully complementary duplexes with canonical base pairing throughout. Only for the most selective pairings, involving C as the 5′-terminal base of the probe, and one pairing with terminal T, did the DNA:RNA cases show more selectivity in hybridization than their DNA:DNA counterparts.

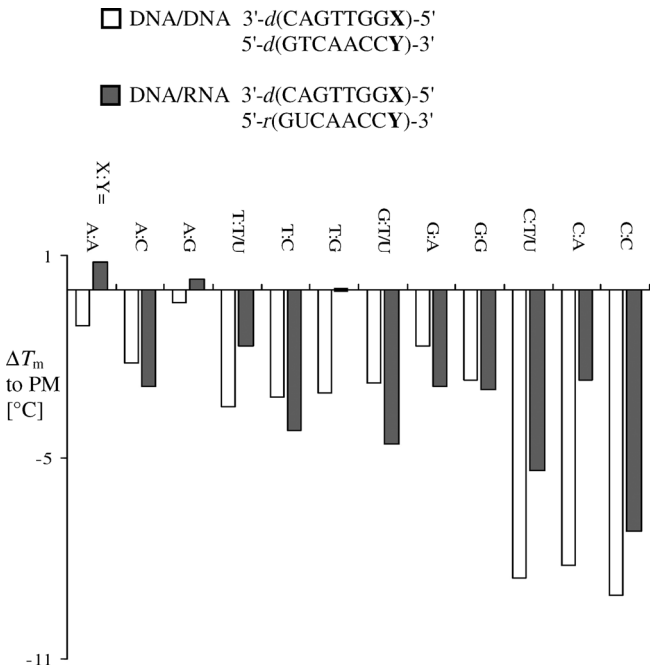

Figure 1. Difference between melting points of DNA:DNA duplexes and DNA:RNA duplexes with terminal mismatch sequences and their corresponding perfectly matched (PM) duplexes. The DNA:DNA duplexes are *d*(**X**GGTTGAC):*d*(GTCAACC**Y**) in which **X** and **Y** stand for the nucleotides given on the bars. The DNA:RNA duplexes are *d*(**X**GGTTGAC):*r*(GUCAACC**Y**). Conditions: phosphate buffer (10 mM, pH 7), NaCl (1 M), and 1.5 μM strand concentration, $\lambda_{det} = 260$ nm.

To better understand the molecular basis of base pairing fidelity and the effect of the backbone structure (ribonucleosides versus deoxyribonucleosides), we decided to extract thermodynamic data from melting curves of duplexes with or without single mismatches at the termini. For this, we used both the current data (Figure 1) and the original melting curves from our earlier work on 3′-caps.[23,20] Other melting point data for longer duplexes with single mismatches (both DNA and RNA), determined on microarrays, can be found in the literature.[24] The enthalpy and entropy of duplex formation were extracted by using the program Meltwin.[25] For each duplex, four individual curves were analyzed and the standard deviation was calculated. The data for each of the four cases (5′-terminus and 3′-terminus for both DNA and RNA target strands) are shown in graphical form in Figure 2a–d. The numerical values can also be found in Tables S6–S9 in the Supporting Information.

As is common for nucleic acid duplexes, there is a very significant enthalpy–entropy compensation. The change of a single base in an octamer duplex does not lead to dramatic changes in the thermodynamic characteristics of the duplex to single-strand transition. Nevertheless, there are some noteworthy trends that can be gleaned from the ΔH and $T\Delta S$ values that together make up the ΔG of duplex formation for each of the duplexes. Firstly, in the vast majority of

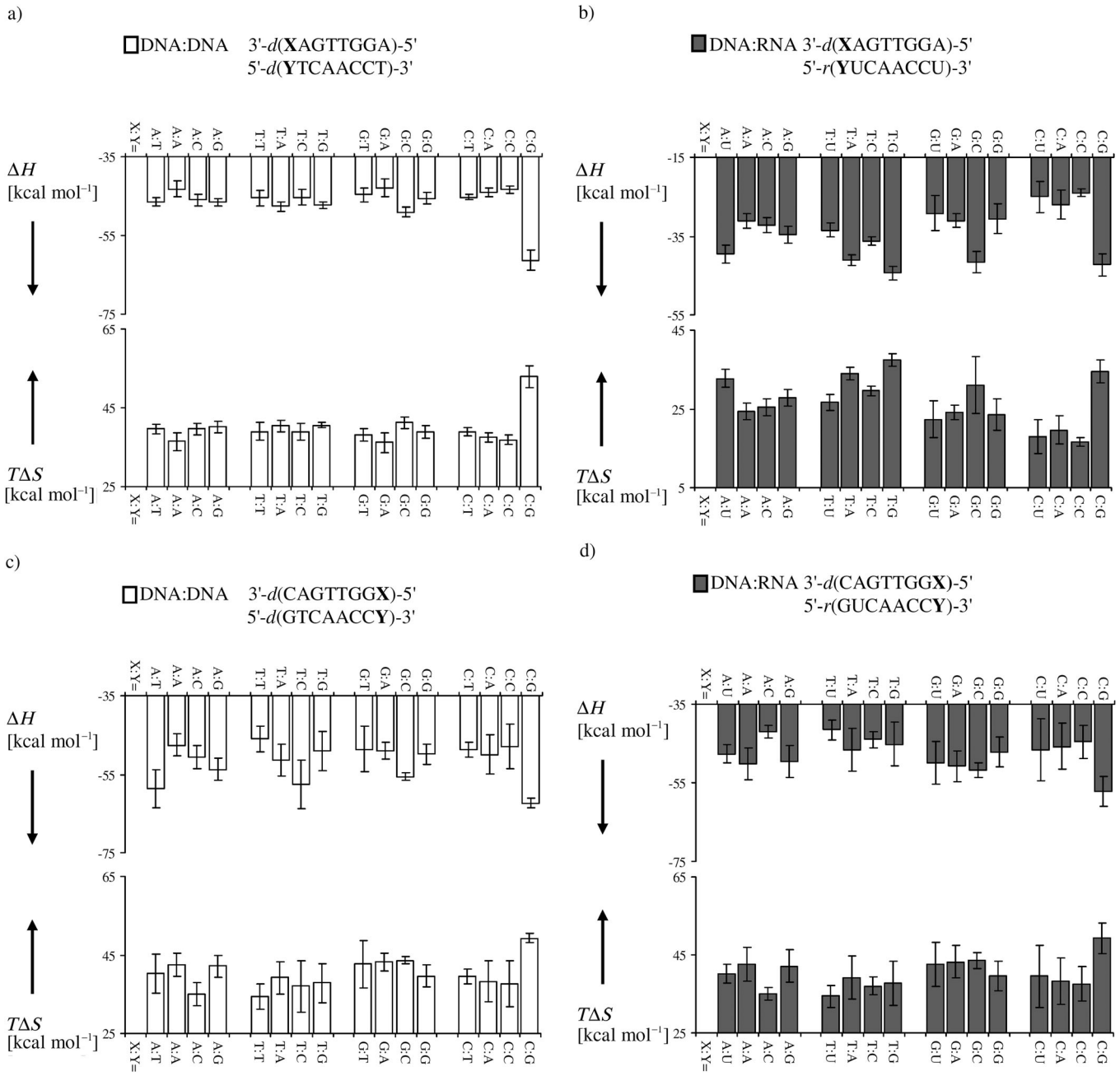

Figure 2. Thermodynamic parameters of duplex formation at 37 °C, as determined from melting curve data by using Meltwin v3.5:[26] a) for the 16 DNA:DNA duplexes *d*(AGGTTGA**X**) and *d*(**Y**TCAACCT), in which **X** and **Y** stand for the nucleotides given above and below the respective bars; b) for the 16 DNA:RNA duplexes of *d*(AGGTTGA**X**) and *r*(**Y**UCAACCU); c) for the 16 DNA:DNA duplexes of *d*(**X**GGTTGAC) and *d*(GTCAACC**Y**); and d) for the 16 DNA:RNA duplexes of *d*(**X**GGTTGAC) and *r*(GUCAACC**Y**). The columns in the upper part of each graph show ΔH values and those in the lower part show $T\Delta S$ values. Thermodynamic data were determined from melting curves detected at 260 nm from a sodium phosphate buffer (10 mM) with NaCl (1 M) and 1.5 μM strand concentration. Note the *y*-axis expansion, chosen to highlight differences.

all cases, the duplexes with perfectly matched bases experience the greatest enthalpic gain upon duplex formation, accompanied by the most significant entropic loss, compared with the mismatch-containing combinations. Secondly, in all but three cases, the enthalpic gain upon duplex formation is smaller when RNA is the target strand than when DNA is the target strand of the octamer probe. Thirdly, the A:A or G:A purine:purine combinations and the G:U wobble base pair are particularly stable cases for the DNA:RNA duplex when a mismatch is found at the 5′-terminus of the probe and the 3′-terminus of the target. For this, the lowest fidelity situation, purines at the 5′-terminus of the probe give the most similar ΔH and $T\Delta S$ values for perfectly matched and mismatch-containing duplexes, that is, the lowest intrinsic capability to generate free energy differences as the basis of selectivity in molecular recognition. Other than this, there

are few truly exceptional compensation phenomena, though, that show an unusually strong enthalpic gain for a mismatched base pairing or a very strong entropic loss upon formation of a canonical base pair. Rather, the formation of a base pair appears to provide an enthalpic gain, whereas the presumed lack of pairing makes duplex formation both enthalpically less favorable and entropically less costly.

However, the data in Figure 1 also show that the base pairing fidelity at the terminus depends strongly on the nucleobase to be detected. For C at the 5′-terminus of the probe, drops in the melting point, caused by a mismatched base in the target, are greatest, whereas for A at the 5′-terminus, discrimination is poorest. When selectivity is poor in the DNA:DNA case, it is poorer still in the DNA:RNA case with RNA as the target strand. As mentioned above, both of the mismatched purine bases in the target give a higher melting point for the duplex with A at the 5′-terminus of the probe than with the matched base, U. This confirms just how difficult it is to achieve fidelity at the 3′-terminus of an RNA target. Whilein the majority of the mismatched cases the DNA:DNA duplex gives a greater enthalpy of formation, the A:A pairing gives a larger ΔH for the DNA:RNA case. This suggests that there are stabilizing interactions not found in sequences with other terminal bases. Inspection of Figures 2c and 2d, in which the corresponding data are presented for binding the other terminus (the 5′-terminus) of the DNA:RNA duplex, makes the phenomenon more conspicuous still. Here, the duplexes with an RNA target strand give lower enthalpy values for duplex formation throughout, even when A is the terminal nucleobase.

It is unlikely that hydrogen bonding is at the core of this difference in selectivity for the two backbones. Rather, differences in the stacking interactions are probably causing the effect. We suspected that the exceptionally high stability of duplexes with 5′-terminal A facing a mismatched A or G in the RNA target was due to bridging interactions that the purine base provides when stacking on the neighboring base pair of the duplex. When RNA is the target strand, an A-form duplex can be expected to form, whereas DNA:DNA duplexes prefer the B-form.[1] The A-form helix possesses a smaller helical pitch (rise per turn) and a smaller helical twist per base pair. This affects the extent to which neighboring bases stack on the nucleobases of a given base pair.

We modeled this situation for terminal nucleotides, assuming that the dangling residue adopts the standard conformation of A- or B-type helices. Figure 3 shows the extent to which a 5′-terminal adenine bridges the duplex in A- and B-form geometries, respectively. A similar image that shows a larger portion of the respective duplexes can be found in the Supporting Information (Figure S1). The adenine bridges the penultimate base pair more extensively in the A-type duplex, making the presence of the complementary base of the target strand less significant for duplex stability. A more detailed analysis of the effect of dangling residues on the stability of DNA and RNA duplexes can be found in the recent literature.[27] This analysis, building on a significant body of earlier work,[28,29] suggests that a dangling 3′-terminal residue of an RNA duplex provides the strongest duplex-stabilizing effect, compared with other dangling nucleotides, so that a stacked 3′-terminal A residue on the target may, by itself, provide much of what a Watson–Crick base pair would provide in duplex-stabilizing effect.

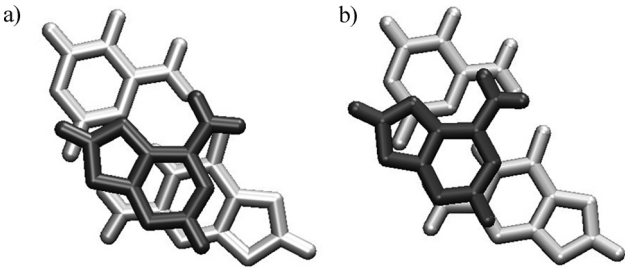

Figure 3. Modeling of the bridging effect of the nucleobase of dangling A residues at the 5′-terminus of duplexes in standard B- or A-form, as expected for DNA:DNA and DNA:RNA duplexes, respectively. The stacking arrangement of the nucleobase of the dangling A (dark grey) and the terminal base pair (light grey) are shown, from a view point along the helix axis. a) Terminus of a DNA:DNA duplex, as generated in silico for the duplex of 5′-**A**CGA-3′ and 5′-TCG-3′. Coordinates were generated with the structure-building tool in Macromodel (version maestro 7.5.106), using default parameters for A-form duplexes. b) Terminus of a DNA:DNA duplex, as generated in silico for the duplex of 5′-**A**CGA-3′ and 5′-UCG-3′ in B-form. Note that for the B-form, the dangling A residue bridges the duplex less than for the A-form.

The shielding effect of 3′-dangling purines on RNA has also been found by NMR[30] and time-resolved spectroscopy.[31] The more strongly bridging the stacking interactions of the 5′-terminal purine base,[28d] and the smaller the remaining stacking surface for the pyrimidine base of the target strand, the less likely it is that formation of the correct, canonical base pair will significantly increase duplex stability. If the 3′-terminal A of the target strand further stacks onto the 5′-terminal A of the probe strand, a zipper-like stacking arrangement could result that reduces the likelihood of duplex dissociation, further adding to what 3′-dangling residues contribute to stability.[32]

Independent of the cause of the poor mismatch discrimination, the lack of selectivity in base pairing for duplexes with a purine at the 5′-terminus of the probe motivates a search for caps as fidelity-enhancing elements more than other constellations in the sequence space of nucleic acids. The cap to be identified should be large enough to provide additional enthalpic gains upon duplex formation. Ideally, the cap should also be universal, stabilizing any of the four canonical base pairs, not just duplexes in which the 5′-terminal base of the probe is a purine, that is, the most difficult case, even for DNA:DNA duplexes.[21] Since destabilizing mismatched pairs is unrealistic, increases in selectivity can most likely be achieved with caps that bind tightly on canonical base pairs, but poorly on mismatched base pairs with different geometries, such as G:U wobble base pairs.[33]

One way to design a cap is to use a dangling *C*-nucleoside with a large aromatic ring as a base surrogate. Such *C*-nucleosides are known for a number of annelated aromatic ring systems, most notably pyrene, and we decided to use a

pyrenyl-*C*-nucleoside[15d,34] as one benchmark compound for our 5′-caps. The other benchmark was an unmodified dangling deoxyadenosine residue.

Synthesis and selection of probes with 5′-caps: Scheme 1, parts a and b show the general design of our cap-bearing strands. Scheme 1c shows the synthesis of the first series of DNA strands with 5′-caps. We selected all-A/T tetradecamer **1** for this series, as a particularly challenging case for the recognition of target strands, forming weak base pairs throughout. The same sequence has previously been employed in our study on isostable DNA:DNA duplexes.[17] Unless a cap showed a significant effect on the duplexes of **1** with the complementary RNA strand, it would not be selected for the second phase, during which optimization was to be performed on an octamer sequence. The shorter duplex resolves more subtle changes in stability, whereas the longer strand gives duplexes more representative of those typically formed on microarrays. All caps feature a terminal stacking moiety for interacting with the nucleobases and a linker unit for connecting the stacking moiety and the phosphodiester at the 5′-terminus of the probe strand. We opted for a flexible alkyl chain to screen for the proper length of the linker. Besides the stacking moiety and linker, the back-

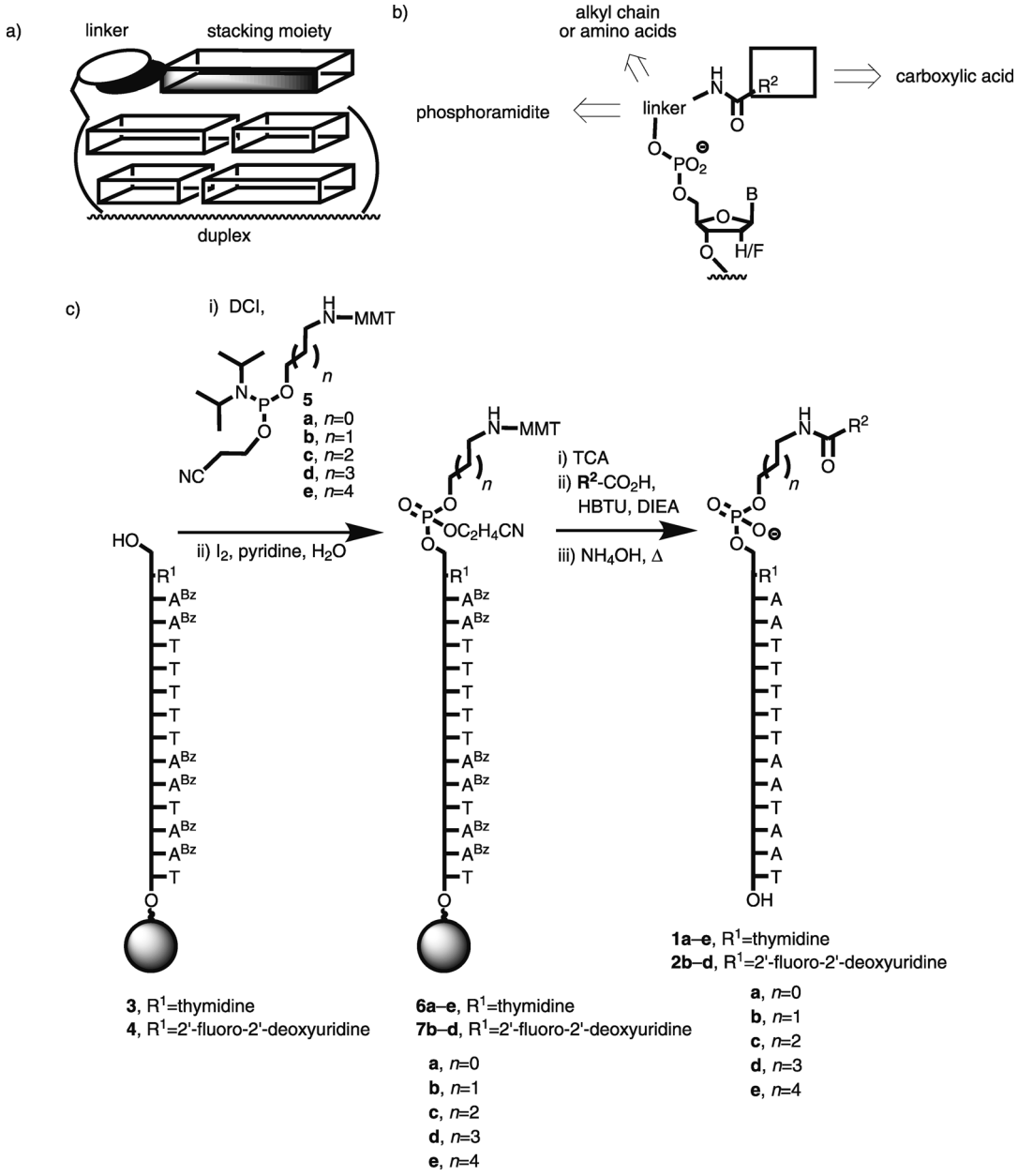

Scheme 1. Cap-bearing oligonucleotides: a) cartoon representation of a duplex with cap, b) retrosynthetic considerations for the assembly of oligonucleotides with caps, and c) synthesis of 5′-capped DNA strands with an all-A/T sequence. Bz = benzoyl; MMT = monomethoxytrityl; TCA = trichloroacetic acid; HBTU = 2-(1*H*-benzotriazole-1-yl)-1,1,3,3-tetramethyluronium hexafluorophosphate; DIEA = *N*,*N*-diisopropylethylamine.

bone of the 5′-terminal nucleotide of the probe was to be varied, with some members of our small library featuring a 5′-terminal 2′-deoxy-2′-fluorouridine residue (general structure **2**), that is, a substitute for thymidine considered to be particularly well suited for binding RNA targets.[12,35]

The assembly of the cap-bearing oligonucleotides started with a conventional DNA synthesis on controlled pore glass, producing supports **3** and **4**. Then, one of five different linker phosphoramidites **5a–e**, with alkyl chains 2–6 methylene groups in length,[36] was coupled to the support (most frequently **5b**), followed by oxidation, yielding supports **6a–e** or **7b–d**. The MMT groups were removed, and the carboxylic acids of potential stacking moieties were coupled under peptide coupling conditions. Cleavage from the solid support with concomitant removal of all protecting groups by treatment with saturated aqueous ammonia gave crude products that were purified by RP–HPLC.

The use of the amino terminal linker allowed for testing of a range of residues of different carboxylic acids as stacking moieties with modest synthetic effort. The stacking moieties chosen are shown in Scheme 2. Some are known to act as molecular caps for DNA:DNA duplexes,[16] others were selected from commercially available carboxylic acids according to the following criteria: 1) the resulting stacking moiety should contain two or more rings for strong stacking interactions with the terminal nucleobases of the DNA:RNA duplex; 2) the acyl residue should contain heteroatoms to avoid excessive lipophilicity and to allow for favorable dipole–dipole interactions with the duplex terminus; and 3) the functional groups should be compatible with oligonucleotide synthesis. The short-hand names of the resulting cap-bearing strands start with the number of the DNA sequence, followed by a lower-case letter (or letters) for the linker and two upper-case letters for the stacking moiety. For example, **1bMS** stands for sequence **1** featuring propyl linker "**b**", to which the acyl group of trimethoxystilbene, "**MS**", is appended (**a** = ethyl, **b** = propyl, **c** = butyl, **d** = pentyl, **e** = hexyl, **f** = aminoethoxyethyl, **t** = 5′-amino-5′-deoxythymidine).

To increase diversity, some phosphoramidites of literature-known or commercial molecular caps were coupled directly to **3**, without the use of a separate linker (Scheme 3). This included the phosphoramidite of pyrenylmethylpyrrolidine (**8**),[21] pyrenylbutanol (**9**),[37] an acridine (**10**), anthraquinoylamido uridine (**11**),[20] and pyrenyl-*C*-nucleoside (**12**),[34] our benchmark compound (see Figure S2 in the Supporting Information for the full structures of **11** and **12**). Coupling and oxidation were again followed by deprotection in aqueous ammonia. In the case of the pyrenyl-*C*-nucleoside, the 5′-hydroxy group was deprotected after HPLC to release fully deprotected pentadecamer **1PC**, whereas for **1AC**, the DMT group was left in place to allow for stacking interactions.

Table 1 lists the UV melting points of duplexes of DNA tetradecamers of general structure **1** with the fully complementary RNA target strand. Compared with the unmodified

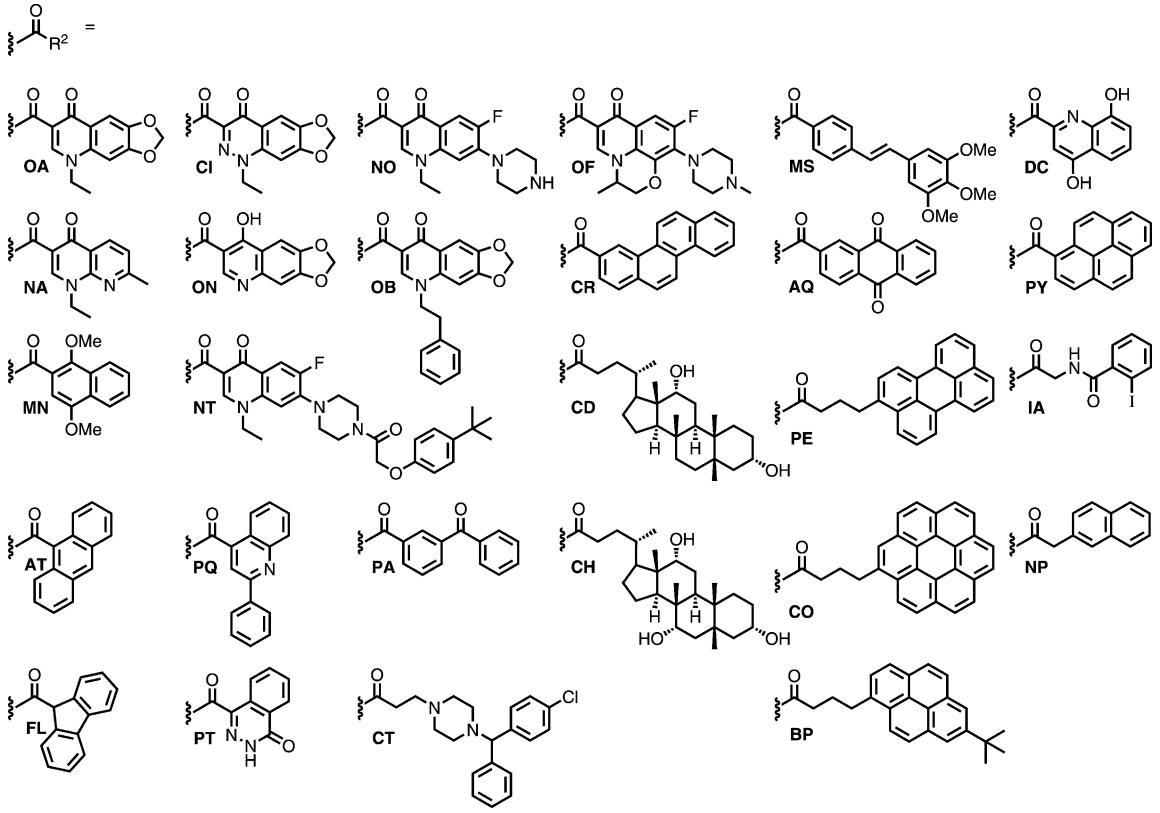

Scheme 2. Carboxylic acid residues of the stacking moieties of molecular caps.

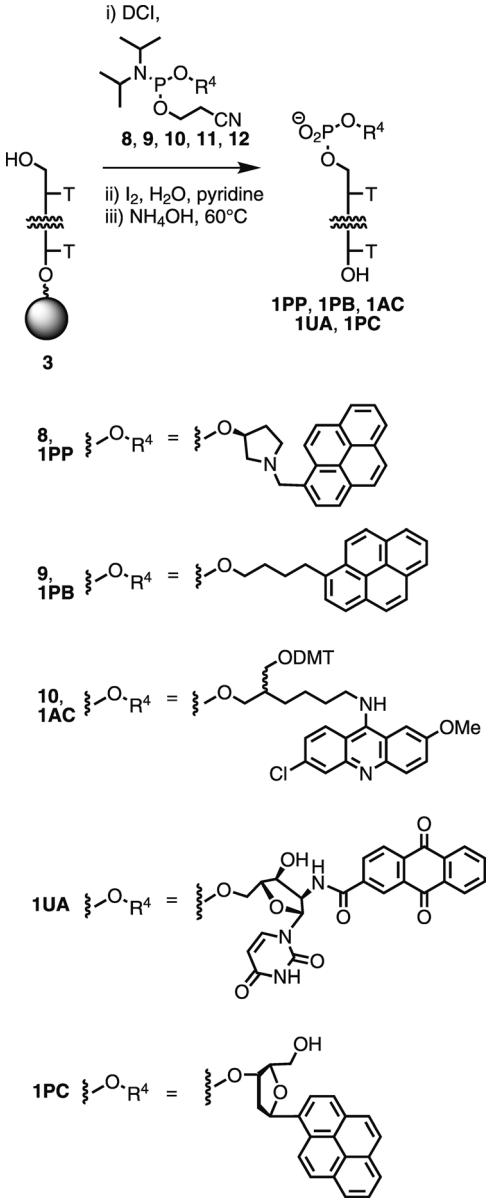

Scheme 3. Synthesis of oligonucleotides with caps introduced through a single phosphoramidite coupling. DMT = 4,4′-dimethoxytrityl.

Table 1. UV melting points for duplexes of DNA tetradecamers of general structure **1** and RNA target strand *r*(AUUAUUAAAAAUUAGUC).

DNA strand	Melting point [°C][a]	ΔT_m [°C][b]	Hyperchromicity [%][c]
1[d]	26.5 ± 1.1	–	29
1A[e]	28.5 ± 0.8	2.0	28
1AC	29.1 ± 0.9	2.6	27
1bMS	27.5 ± 0.9	1.0	31
1PB	26.1 ± 1.4	−0.4	23
1PP	22.9 ± 0.7	−3.6	14
1bCR	29.6 ± 0.8	3.1	29
1fCR	27.0 ± 0.9	0.5	30
1tCR	27.1 ± 0.7	0.6	28
1bAQ	28.5 ± 0.7	2.0	24
1tAQ	27.8 ± 0.9	1.8	27
1UA	29.0 ± 0.8	2.5	30
1bPQ	26.8 ± 1.3	0.3	32
1bAT	25.5 ± 0.5	−1.0	30
1bPY	27.5 ± 0.5	1.0	33
1tPY	26.4 ± 1.0	−0.1	28
1bCH	25.0 ± 0.6	−1.5	31
1bCD	26.0 ± 1.0	−0.5	33
1tBP	22.2 ± 1.0	−4.3	23
1bMN	28.0 ± 1.1	1.5	31
1bIA	27.3 ± 0.8	0.8	34
1bPT	27.0 ± 1.0	0.5	34
1bFL	27.0 ± 1.0	0.5	35
1bPA	26.3 ± 0.8	−0.2	32
1bNP	26.0 ± 1.0	−0.5	32
1bCT	25.5 ± 1.0	−1.0	31
1bDC	26.3 ± 1.1	−0.2	32
1bPE	25.7 ± 1.0	−0.8	30
1fPE	25.0 ± 0.9	−1.5	31
1bCO	25.4 ± 0.9	−1.1	26
1fCO	25.1 ± 1.0	−1.4	24
1bCI	29.6 ± 0.7	3.1	31
1bNA	28.1 ± 0.8	1.6	30
1bOF	26.9 ± 1.0	0.4	32
1bOA	30.7 ± 1.0	4.2	30
1fOA	27.9 ± 1.0	1.4	30
1tOA	30.8 ± 0.8	4.3	31
1PC	31.7 ± 0.7	5.2	31
1ogOA	36.2 ± 0.8	9.7	28

[a] Average of four melting points at 1 μM strand concentration in phosphate buffer (10 mM, pH 7) and NaCl (1 M). [b] Melting point difference to unmodified control duplex of **1** with *r*(AUUAUUAAAAAUUAGUC). [c] Hyperchromicity of the thermal transition, measured at 260 nm. [d] Unmodified DNA control strand. [e] Unmodified DNA strand *d*(ATAATTTTTAATAAT) with dangling dA residue at the 5′-terminus.

duplex, most duplexes of cap-bearing strands gave a modest increase in melting point. However, in a few cases, the ΔT_m value was negative, suggesting that the cap reduced the propensity of the DNA strand to engage in duplex formation, possibly by favoring alternative structures or interfering with base pairing. The ΔT_m value for the duplex featuring benchmark pyrenyl-*C*-nucleoside **1PC** was found to be +5.2 °C. The otherwise unmodified DNA:RNA duplex with a 5′-dangling dA residue as the molecular cap (**1A**) gave an increase in melting point of +2.0 °C, that is, less than could have been expected based on the data on longer RNA duplexes with dangling residues.[38] Melting point increases for **1bPY**, **1bAQ**, and **1bMS** were no more than 1.0–2.0 °C. Strands featuring caps **AC**, **PP**, **PB**, and **UA**, introduced in one step as phosphoramidites, induced no more than a small melting point increase. This was also true for caps known to strongly stabilize DNA:DNA duplexes, like pyrenylmethylpyrrolidine (**PP**),[21] anthraquinone-bearing uridine (**UA**),[20] and trimethoxystilbene (**MS**),[19e] which all had a small effect on the stability of the DNA:RNA duplex studied. For example, the duplex of trimethoxystilbene-bearing **1bMS** with the RNA complement gave a ΔT_m value of +1.0 °C. The corresponding DNA:DNA duplex of the same length gives +5.4 °C under the same conditions.[17] This demonstrates the strong effect of the backbone of the target strand on the stabilizing effect of caps. However, the salt dependence of the melting point did not show unusual effects (see Table S3 in the Supporting Information for melting points at 150 mM

NaCl), and subsequent experiments were run at 1 M NaCl only, as microarray experiments are typically performed at high salt concentrations.[39]

Chrysene has previously been proposed as a particularly well-suited stacking moiety.[22b] The duplex of chrysene-bearing **1bCR** gave a ΔT_m value of +3.1 °C, but other large polycyclic aromatic ring systems, like perylene, coronene, *tert*-butylpyrene, anthracene, and 2-phenyl-4-quinoline, did not stabilize the DNA:RNA duplex (strands **1bPE**, **1bCO**, **1tBP**, **1bAT**, and **1bPQ**, respectively). Bile acid residues (**1bCH** and **1bCD**) also failed to increase duplex melting points. Most stacking moieties with just two aromatic rings (**1bMN**, **1bIA**, **1bPT**, **1bFL**, **1bPA**, **1bNP**, **1bCT**, and **1bDC**) also fared poorly. The most encouraging results were obtained for chinolones as stacking moieties. The duplex with the residue of oxolinic acid (**1bOA**) gave a ΔT_m value of +4.2 °C, just shy of the value for the pyrenyl benchmark cap. The structural details of the chinolone ring system did have an effect, though, with cinoxacine inducing a ΔT_m value of +3.1 °C (**1bCI**, isoelectronic to **1bOA**), whereas bicyclic nalidixic acid (**1bNA**) and tetracyclic ofloxacine (**1bOF**) provided little duplex stabilization.

Table 2 lists melting points of duplexes of eight other versions of **1** or **2** with the complementary RNA target strand. Two features were varied among these probes: the length of the alkyl chain of the linker (**1aOA**–**1eOA**) and the structure of the 5′-terminal nucleotide residue (**2bOA**–**2dOA**). For conventional, 5′-thymidyl DNA **1**, the optimum linker length, as defined by the highest melting point, was four (**1cOA**) or five methylene units (**1dOA**). For the strands with a 5′-terminal 2′-fluorouridine (**2**), higher overall melting values were recorded, and slightly longer alkyl chains appeared more favorable (Figure 4). The additional increase in duplex melting point when the 5′-terminal thymidine was replaced by a 2′-fluoro-2′-deoxyuridine residue (**2bOA**–**2dOA**) again pointed to an important role of backbone structure at the terminus on the stability of the duplex. We noted this, but did not pursue 2′-fluoronucleosides themselves further, as this would require four different cap phosphoramidites, one for each possible 5′-terminal base (A/C/G/T), in probes to be synthesized for practical applications, making the synthesis more costly and the use of caps less attractive.

Table 2. UV melting points for duplexes of DNA tetradecamers **1** or **2** with the residue of oxolinic acid as the stacking moiety, linked by alkyl chains of different length, and target RNA strand *r*(AUUAUUAAAAAUUAGUC).

Strand	Melting point [°C][a]		ΔT_m	Hyperchromicity
	[NaCl] = 150 mM	[NaCl] = 1 M	[°C][b]	[%][c]
1[d]	21.0 ± 0.9	26.5 ± 1.1	–	29
1aOA	18.5 ± 1.0	27.0 ± 1.0	0.5	28
1bOA	22.4 ± 1.1	30.7 ± 1.0	4.2	30
1cOA	23.2 ± 1.1	31.2 ± 0.9	4.7	29
1dOA	23.2 ± 1.1	31.3 ± 0.8	4.8	30
1eOA	22.8 ± 1.1	30.8 ± 0.8	4.3	33
2bOA	22.3 ± 0.7	31.5 ± 0.5	5.0	29
2cOA	26.4 ± 1.0	35.1 ± 0.8	8.6	35
2dOA	27.4 ± 0.7	35.7 ± 0.7	9.2	35

[a] Average of four melting points at 1 μM strand concentration at the NaCl concentration given and in sodium phosphate buffer (10 mM, pH 7). [b] Melting point difference to unmodified control duplex *d*(TAATTTTTAATAAT):*r*(AUUAUUAAAAAUUAGUC). [c] Hyperchromicity upon duplex dissociation at 1 M NaCl. [d] Unmodified DNA with control sequence.

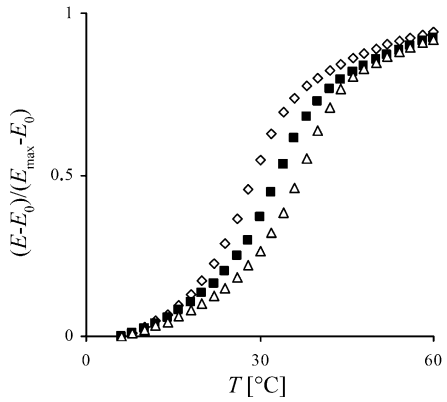

Figure 4. Representative melting curves of duplexes with or without a molecular cap. Perfectly matched DNA:RNA duplexes with RNA target strand *r*(CUG**A**UUAAAAAUUAUUA) and DNA strands *d*(**T**AATTTTTAATAAT) (**1**, ◇, control) or cap-bearing **1dOA** (■) and **2dOA** (△).

Optimization of the linker of the 5′-cap: We then proceeded to vary the linker structure, using the residue of oxolinic acid as the stacking moiety. First, two heteroatom-containing linkages were tested, by using phosphoramidites **13** and **14** (Scheme 4). One features a flexible backbone and a single oxygen atom in the chain (**1fOA**), and one the 5′-amino-5′-deoxythymidine linker known from the 'composite cap' of our earlier work on DNA:DNA duplexes (**1tOA**).[40] The former gave an inferior duplex-stabilizing effect, compared to its alkyl counterpart **1bOA** (Table 1). The latter gave a ΔT_m value similar to that of the duplex of **1bOA**, even though the linkers are not structurally similar. For chrysene

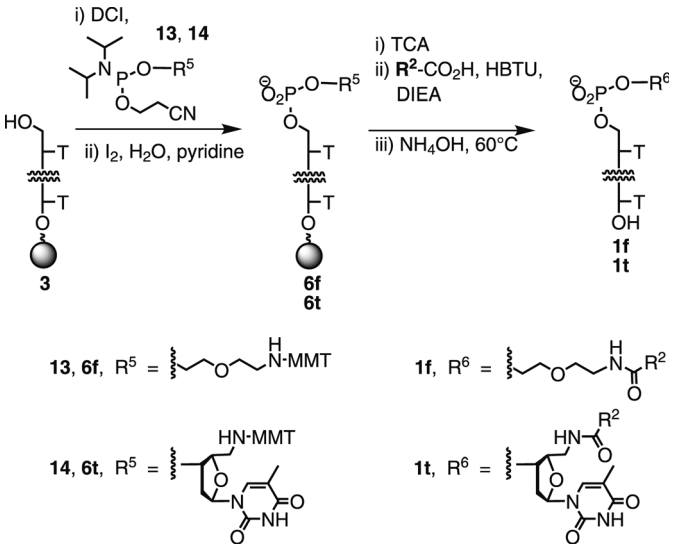

Scheme 4. Synthesis of cap-bearing oligonucleotides with unconventional linkers.

as the stacking moiety, either linker led to a melting point depression in comparison with linker **b** (**1fCR** and **1tCR** versus **1bCR**). For other combinations of stacking moieties and linkers **f** and **t**, we also observed no duplex stabilization (**1tAQ**, **1tPY**, **1fPE**, and **1fCO**). This suggested that we were still far from a local optimum in linker structure. Since the base pairs at the termini themselves are similar in DNA:DNA and DNA:RNA duplexes, and the T_m values did not come close to those observed for our optimized DNA:DNA 5′-caps,[19e,21,40] a further "walk" in the structure space of linkers seemed the most logical step. Furthermore, it seemed reasonable to construct linkers with at least one ring structure.

Prior to linker optimization, we asked whether the C5-linked cap **dOA** was suitable for stabilizing all of the four canonical Watson–Crick base pairs (A:U, T:A, C:G, and G:C). For this, we switched to octamer sequence 5′-**B**GGTTGAC-3′, with **B** = A/C/G/T, partly because we were necessarily leaving the all-A/T sequence space in this phase, partly because the melting point of shorter sequences is more sensitive to small changes in structure, making it easier to optimize structures. Sequences with any of the four possible terminal nucleobases were generated (**15dOA**–**18dOA**), starting from supports **19**–**22** (Scheme 5). These were reacted with phosphoramidite **5d**, and subsequently acylated with the active ester of oxolinic acid. The data listed in the middle portion of Table 3 show that strong melting point increases are induced for each of the possible terminal base pairs, with ΔT_m values ranging from +8.1 to + 12.1 °C. However, a crucial test for mismatch discrimination, namely the melting curve for the duplex with a terminal A:A mismatch, gave an unsatisfactory result for cap **dOA** (Table 4). No more than a marginal increase in the ΔT_m value compared to the perfectly matched counterpart was observed, confirming the need for a linker that preorganizes the stacking moiety towards interacting with the correct terminal bases.

Table 3. UV melting points of perfectly matched DNA:RNA duplexes for the four possible terminal base pairs, with or without a 5′-DNA cap.

DNA strand	RNA target strand	T_m [°C][a]	ΔT_m[b]
d(**A**GGTTGAC)	*r*(GUCAACC**U**)	31.2	–
d(**T**GGTTGAC)	*r*(GUCAACC**A**)	30.4	–
d(**G**GGTTGAC)	*r*(GUCAACC**C**)	34.8	–
d(**C**GGTTGAC)	*r*(GUCAACC**G**)	34.4	–
15dOA	*r*(GUCAACC**U**)	39.3	+8.1
16dOA	*r*(GUCAACC**A**)	40.3	+9.9
17dOA	*r*(GUCAACC**C**)	46.9	+12.1
18dOA	*r*(GUCAACC**G**)	44.6	+10.2
15ogOA	*r*(GUCAACC**U**)	38.5	+7.3
16ogOA	*r*(GUCAACC**A**)	42.6	+12.2
17ogOA	*r*(GUCAACC**C**)	47.9	+13.1
18ogOA	*r*(GUCAACC**G**)	45.7	+11.3

[a] Average of four melting points at 1 μM strand concentration in sodium phosphate buffer (10 mM, pH 7) and NaCl (1 M). The standard deviation of four measurements was between ±0.2 and ±1.1 °C. [b] Melting point difference to the unmodified, perfectly matched control duplex of the same sequence.

We reasoned that a more rigid linker would prevent the stabilization of duplexes with anything but the desired Watson–Crick geometry at the terminus. The most attractive approach to optimizing the linker was to employ peptide chemistry. To install a rigidifying ring structure, we based linkers on L-prolinol. Target strands of the sequences **15**–**18** were assembled on supports **19**–**22**, through coupling with phosphoramidite **23**, followed by oxidation to give **24**–**27** (Scheme 5). The Fmoc-terminated chain was then deprotected, acylated with the Fmoc-protected residue of a second amino acid, which was then relieved of its Fmoc group, followed by coupling of the activated form of the carboxylic acid of the stacking moiety (usually the active ester of oxolinic acid).

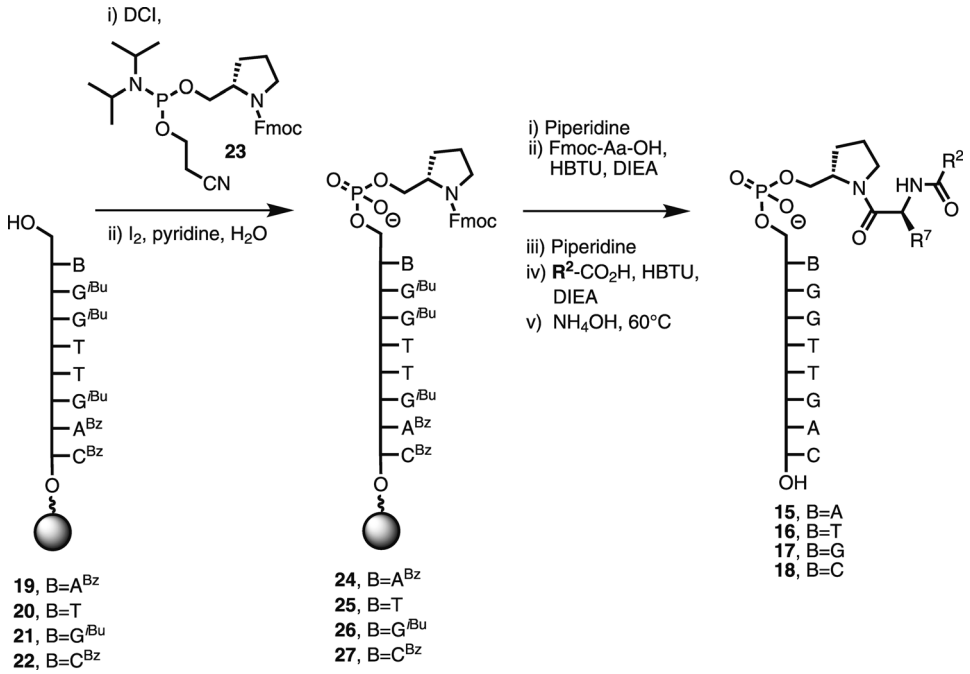

Scheme 5. Representative synthesis of 5′-capped DNA octamers by phosphoramidite coupling with building block **23**, followed by amide-forming couplings with an amino and/or carboxylic acid by using peptide chemistry. Fmoc = fluorenylmethyloxycarbonyl; *i*Bu = isobutyryl.

Scheme 6 shows an overview of the amino acid residues tested as parts of the linker. The list includes D- and L-prolinol (**o** and **r**, respectively), hydroxyprolinol with or without the bulky terminal DMT group (**h** and **j**, respectively), and a cyclohexyl moiety (**x**). The structures and syntheses of linker phosphoramidites **28**–**30**, used

Table 4. UV melting points for duplexes of DNA octamers with the oxolinic acid cap linked by different linkers and the perfectly-matched (PM) target RNA strand *r*(GUCAACC**U**) or target strand *r*(GUCAACC**A**) with a terminal A:A mismatch next to the molecular cap (MM = mismatched).

DNA strand	RNA strand *r*(GUCAACC**U**)		RNA strand *r*(GUCAACC**A**)	
	T_m[a] [°C]	PM ΔT_m[b] [°C]	T_m[a] [°C]	MM ΔT_m[c] [°C]
d(**A**GGTTGAC)	31.2	–	32.0	+0.8
d(**AA**GGTTGAC)	32.8	+1.6	32.3	−0.5
15dOA	39.3	+8.1	39.1	−0.2
15ogOA	38.5	+7.3	34.1	−4.4
15opOA	30.6	−0.6	31.3	+0.7
15bpOA	31.0	−0.2	30.1	−0.9
15owOA	35.1	+3.9	34.2	−0.9
15oOA	32.0	+0.8	31.5	−0.5
15ovOA	36.8	+5.6	34.8	−2.0
15ouOA	36.5	+5.3	35.4	−1.1
15oggOA	31.8	+0.6	33.7	+1.9
15osOA	31.0	−0.2	31.5	+0.5
15oyOA	30.8	−0.4	31.7	+0.9
15ozOA	31.6	+0.4	31.8	+0.2
15hgOA	38.3	+7.1	33.4	−4.9
15jgOA	38.3	+7.1	34.3	−4.0
15rOA	32.3	+1.1	31.9	−0.4
15rgOA	38.4	+7.2	34.7	−3.7
15xOA	31.0	−0.2	35.8	+4.8
15xgOA	29.2	−2.0	32.5	+3.3
15xuOA	<15	–	<15	–

[a] Average of four melting points at 1.5 μM strand concentration in sodium phosphate buffer (10 mM, pH 7) and NaCl (1 M). [b] Melting point difference to unmodified control duplex *d*(**A**GGTTGAC):*r*(GUCAACC**U**). [c] Melting point difference to the corresponding modified perfectly matched duplex.

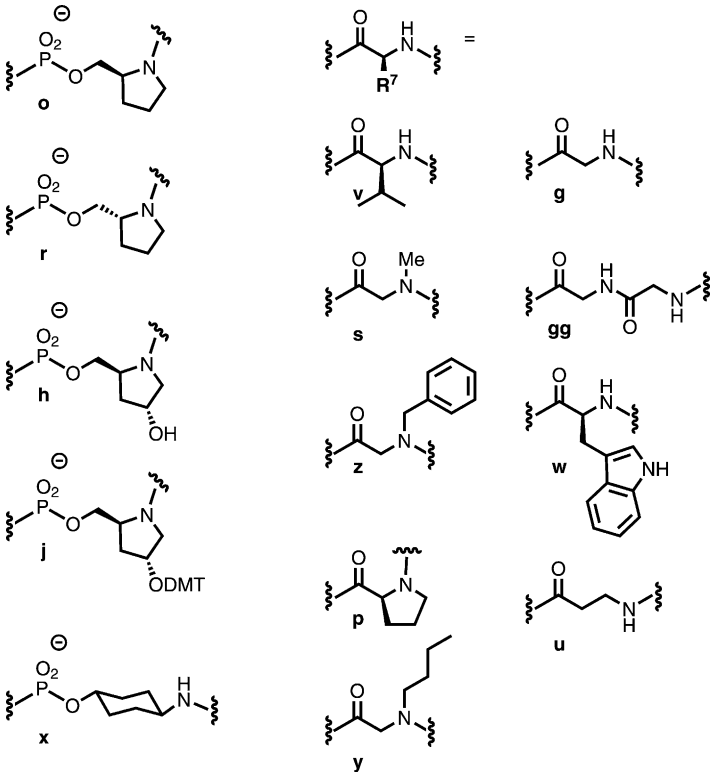

Scheme 6. Amino acid residues employed in the optimization of the linker at the 5′-terminus of the DNA chain and stacking moieties that were based on peptide chemistry. The stacking moieties are shown in Scheme 2.

to introduce linkers **o**, **r**, **h**, **j**, and **x**, are shown in the Supporting Information (Figure S2 and Scheme S1 in the Supporting Information). The proximal amino alcohols of the linkers were combined with amino acids like β-alanine for increased chain length (**u**) or α-amino acid residues with (**v** and **w**) or without side chains (**g** and **gg**), with an additional ring structure (**p**), or with substituents on the backbone nitrogen (**s**, **y**, and **z**) to produce a diverse set of linkers. Table 4 shows the melting points of duplexes of the resulting probe strands with the complementary RNA target, as well as the RNA target producing a terminal A:A mismatch. We assayed duplex stability for this most problematic terminal mismatch throughout to obtain at least one data point on fidelity early on. Compared to a dangling dA residue as the cap, which gives a ΔT_m value of +1.6 °C for the perfectly matched (PM) duplex and a slight decrease in the ΔT_m value for the terminal A:A mismatch (−0.5 °C), a number of caps showed an improvement. From the range of combinations, prolinol with glycine emerged as the most duplex-stabilizing, giving a perfect match ΔT_m value of +7.3 °C. Neither a longer linker, as produced by the combination of prolinol with β-alanine (**1ouOA**), nor prolinol with two glycine units (**1oggOA**), nor a shorter linker, like prolinol alone (**1oOA** or **1rOA**), led to greater duplex stabilization than **ogOA**, which provided the best combination of affinity and selectivity (Table 4).

We also tested the combination of propylene linker **b** with proline, but the resulting strand **15bpOA** did not show an increase in T_m. The same was true for prolinol followed by proline (**1opOA**), suggesting that the attachment of the stacking moiety through a cyclic amino acid is disadvantageous. The strands with prolinol and side-chain-bearing α-amino acid residues, such as valine (**1ovOA**) or tryptophane (**1owOA**), gave ΔT_m values of +5.6 and +3.9 °C, respectively, for the matched duplex, whereas all three *N*-substituted amino acid linkers (**15osOA**, **15oyOA**, and **15ozOA**) gave disappointing results. Apparently, a side chain on the amide nitrogen of the second residue interferes with the productive binding of the molecular cap. Probe strands with cyclohexyl linker **x**, with or without glycine or β-alanine residue (**1xOA**, **1xgOA**, and **1xuOA**), did not show any duplex-stabilizing effect on the PM duplex, but stabilized MM duplexes with a terminal A:A mismatch. When prolinol was replaced by hydroxyprolinol (**1hgOA**) or its DMT-bearing counterpart (**1jgOA**), the same effect on the T_m value as for cap **ogOA** was measured, both for the PM and the MM case. This was also largely true for a cap containing D-prolinol (**1rgOA**), which gave a perfect match ΔT_m value of +7.2 °C and a slightly decreased mismatch ΔT_m value of −3.7 °C. This suggested that the prolinol portion of the linker, while sensitive to structural changes, tolerates substituents more readily than the glycine residue in the **ogOA** cap.

Having refined the linker, we then revisited the stacking moiety one last time. Quinolones other than oxolinic acid were coupled to the amino-terminal strand featuring the **og** linker, followed by deprotection, purification, and melting curve assays with complementary strands (Table 5). Again, the most problematic mismatched base combination at the terminus (A:A) was also assayed. The results in Table 5 show that **ogOA** itself is the most favorable cap for inducing both target affinity and base pairing selectivity. Of the other chinolones tested, only cinoxacine was again found as a possible replacement for oxolinic acid as the stacking moiety, although the T_m value was slightly decreased for **15ogCI**, and so was the effect on mismatch discrimination for the terminal A:A mismatch. The remaining residues of chinolones tested, like ofloxacine, nalidixic acid, and norfloxacine, gave smaller duplex stabilizing effects (**15ogOF**, **15ogNA**, and **15ogNO**, respectively). In order to couple norfloxacine to the amino terminus of the linker, the secondary amine of the quinolone was acylated with *tert*-butylphenoxyacetic acid (see Scheme S3 in the Supporting Information). Partial deprotection of the resulting strand during cleavage from the solid support allowed us to test both the acylated and non-acylated forms (**15ogNT** and **15ogNO** , respectively). We also tested more distantly related stacking moieties like anthraquinone, pyrene, and trimethoxystilbene in combination with the **og** linker, but neither **15ogAQ**, **15ogPY**, nor **15ogMS** induced higher melting points than **15ogOA**. An extended version of the ethyl side chain of oxolinic acid (the phenylethyl group in **OB**, Scheme 2) was tested by alkylating ethyl-8-hydroxy[1,3]dioxolo[4,5-g]chinoline-7-carboxylate,[41] and treating the product with sodium hydroxide to give the carboxylate of **OB** (see Scheme S2 in the Supporting Information). The resulting modified DNA strand **15ogOB** showed very similar duplex stability to **15ogOA** when hybridized to its complementary RNA strand, but no increase in melting point. The non-alkylated species **ON** was also tested as a stacking moiety (**15ogON**). It gave a slightly decreased duplex melting point compared with **15ogOA**. This suggested that the side chain of **OA** makes some contacts, but is not critical for the effectiveness of the cap.

Table 5. UV melting points for duplexes of DNA octamers with different stacking moieties and the prolinol glycine linker and perfectly matched target RNA strand *r*(GUCAACC**U**) or target strand *r*(GUCAACC**A**) producing a terminal A:A mismatch.

DNA strand	RNA strand *r*(GUCAACC**U**)		RNA strand *r*(GUCAACC**A**)	
	T_m [°C][a]	PM ΔT_m [°C][b]	T_m [°C][a]	MM ΔT_m [°C][c]
d(**A**GGTTGAC)	31.2	–	32.0	+0.8
15ogOA	38.5	+7.3	34.1	−4.4
15ogOF	34.0	+2.8	35.1	+1.1
15ogAQ	37.8	+6.6	37.4	−0.4
15ogPY	34.4	+3.2	34.4	0.0
15ogMS	35.6	+4.4	32.0	−3.6
15ogNA	36.1	+4.9	32.1	−4.0
15ogCI	38.3	+7.1	34.4	−3.9
15ogNO	34.7	+3.5	34.0	−0.7
15ogNT	32.6	+1.4	33.1	+0.5
15ogON	37.6	+6.4	34.2	−3.4
15ogOB	38.1	+6.9	33.8	−4.3

[a] Average of four melting points at 1.5 μM strand concentration in sodium phosphate buffer (10 mM, pH 7) and NaCl (1 M). [b] Melting point difference to unmodified control duplex *d*(AGGTTGAC):*r*(GUCAACCU). [c] Melting point difference to the corresponding modified perfectly matched duplex.

Having settled on **ogOA** as the cap, we tested for stabilization of any of the four canonical terminal Watson–Crick base pairs (A:U, T:A, C:G, and G:C). For this, we synthesized DNA octamers **15ogOA**–**18ogOA** (Scheme 5) and measured melting points of the duplexes with RNA target strands (lower part of Table 3). Compared with the unmodified DNA:RNA control duplexes, melting point increases of 7.3–13.1 °C were found. Figure 5 shows an overlay of melting curves of perfectly matched and mismatch-containing duplexes with and without the **ogOA** cap. The melting point of the capped, perfectly matched duplex **18ogOA**:**32** is massively increased over that of to the unmodified duplex (**31**:**32**, filled symbols), but the duplex with a terminal C:C mismatch does not experience stabilization by the cap (**31**:**33** and **18ogOA**:**33**, open symbols).

The improvement in fidelity achieved with the peptidic linker in **ogOA** over the alkyl linker in **dOA** was even more apparent when the entire matrix of melting points of duplexes with terminal mismatches was measured. Figure 6 shows the drop in duplex melting point for a 3′-terminal, mismatched nucleobase in the RNA strand compared to the fully matched duplexes. Although either cap improved discrimination for all of the twelve terminal mismatches, compared to the unmodified DNA:RNA duplexes, the effect was considerably stronger for **ogOA** in every case. Significant selectivity was now observed even for the cases for which the mismatch gives a more stable duplex than the perfect match in the unmodified control duplexes (A:A and A:G, Figure 1). For the absolute melting points of the entire 4×4 matrix of base combinations at the terminus, see Table S4 in the Supporting Information. In the most favor-

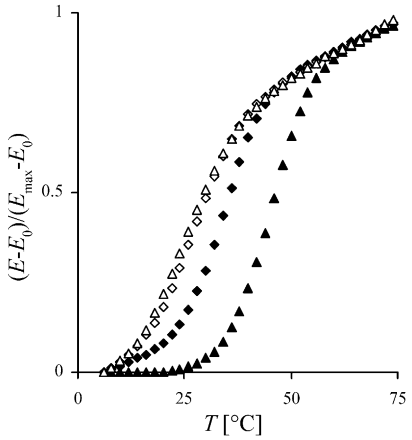

Figure 5. Representative melting curves of duplexes with or without a molecular cap. Melting curves of octamer DNA:RNA duplexes either without *d*(**C**GGTTGAC) (**31**) or with cap (**18ogOA**), and either containing no *r*(GUCAACC**G**) (**32**), or one terminal C:C mismatch, *r*(GUCAACC**C**) (**33**). Key: ◆= **31**:**32**, ◇=**31**:**33**, ▲=**18ogOA**:**32**, △= **18ogOA**:**33**.

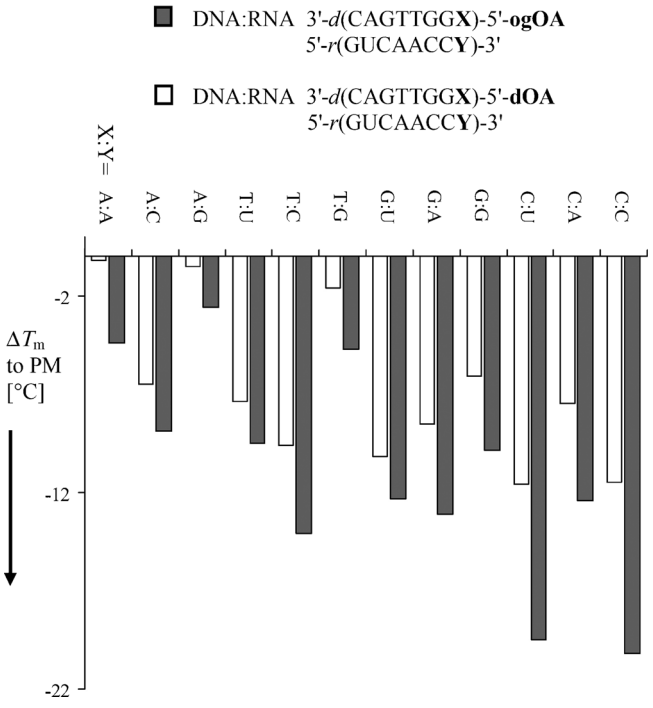

Figure 6. Difference between melting points of two types of capped DNA:RNA duplexes with terminal mismatches and those of the corresponding perfectly matched duplexes (compare Table 3). The capped DNA:RNA duplexes consist of the strands **15dOA**, **16dOA**, **17dOA**, **18dOA**, **15ogOA**, **16ogOA**, **17ogOA**, **18ogOA**, and *r*(GUCAACC**Y**), in which **Y** stands for one of the four nucleosides (A, C, G, or T/U). Melting curve data was determined from a sodium phosphate buffer (10 mM) with NaCl (1 M) and 1.5 μM strand concentration, detected at 260 nm.

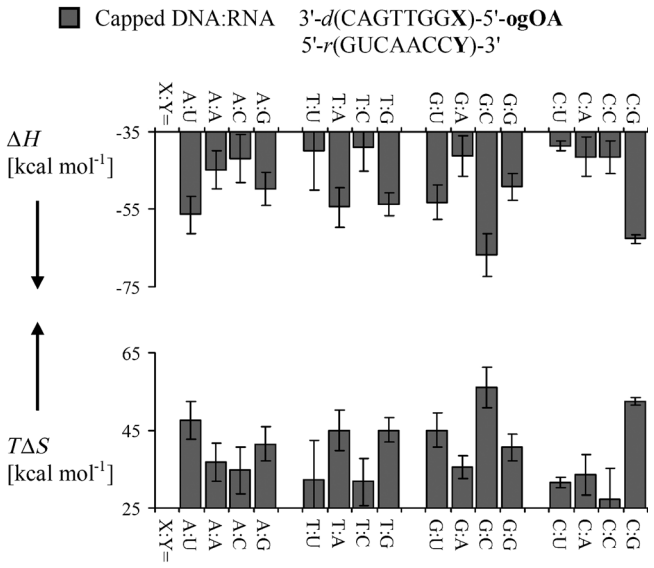

Figure 7. Thermodynamic parameters for DNA:RNA duplex formation at 37 °C, as determined from melting curve data by using Meltwin v3.5.[26] The modified DNA:RNA duplexes feature **15ogOA**, **16ogOA**, **17ogOA**, and **18ogOA** as the probe strands and *r*(GUCAACC**Y**), in which **Y** is one of the four possible nucleotides, as the target. The columns in the upper part of the graph show ΔH at 37 °C and in the lower part the values for $T\Delta S$ at 37 °C are shown. Data from curves detected at 260 nm from a solution with sodium phosphate buffer (10 mM), NaCl (1 M), and 1.5 μM strand concentration. Note the absolute expansion of the *y*-axis chosen to highlight differences.

able cases, for which strong hydrogen bonds and proper dipole–dipole interactions provide a high level of selectivity, as for C:G base pairs,[42] the drop in melting point for a mismatch went up to −20.2 °C (for the C:C mismatch, compared with the C:G perfect match) in the presence of cap **ogOA**. Selectivity thus reached a level similar to that of the very best caps for DNA:DNA duplexes[19e] or the 3′-terminal cap of DNA:RNA duplexes published recently.[20]

Further confirmation of the desired effect of the **ogOA** cap on DNA:RNA duplexes came from a thermodynamic analysis of the melting transitions (Figure 7). Absolute values can be found in Table S10 in the Supporting Information. The cap increases the enthalpic gain upon formation for perfectly matched duplexes by 5.5 to 15.1 kcal mol^{-1}, compared with the unmodified duplexes (Figure 2d). For mismatch-terminated duplexes, the gain is significantly smaller. For G:U and G:G mismatch-containing duplexes, the cap induces a gain of just 2.1–3.4 kcal mol^{-1}, and for the critical A:A base combination, it gives just −5.3 kcal mol^{-1} compared to the unmodified duplex. The enthalpic gains are accompanied by a significant, but not overwhelming loss of entropy. The $T\Delta S$ for the capped duplexes decreases, whereas it remains essentially unchanged for others. In the case of the terminal C:C mismatch, the decrease in $T\Delta S$ reaches 10.3 kcal mol^{-1} compared with the unmodified duplex, confirming a favorable enthalpy–entropy compensation.

Gratifyingly, cap **ogOA** also performed well on the tetradecamer sequence **1**, with a melting point increase of +9.7 °C for the duplex of this long all-A/T probe (**1ogOA**) with its matched RNA target compared with the unmodified control (last entry in Table 1). This value compares favorably with that of optimized caps for DNA:DNA, such as the trimethoxystilbene cap,[17] which increases the melting point of the all-A/T tetradecamer by +5.4 °C. Finally, and perhaps most importantly, the cap also fared well when tested as a fidelity-enhancing element in a focused hybridization probe detecting one member of a family of medically relevant miRNAs, let7a (**34**),[43,44] versus a closely related miRNA, let7c (**35**), for which unmodified DNA does not. Figure 8 shows melting curves for duplexes between DNA probes, **36** and **37**, and miRNA, let7c (**35**) and let7a (**34**). In the case of the unmodified, full-length hybridization probe (**38**), melting points of duplexes with either target are virtually indistinguishable, with a melting-point difference of just 1.8 °C, whereas the cap-bearing probe binds selectively, with a ΔT_m value of +9.2 °C (for full T_m values, see Table S5 in the Supporting Information).

Discussion

The termini of duplexes are critical sites for base pairing, as dissociation of short duplexes typically starts with fraying at the termini. However, the termini are also the sites of pivotal genetic processes. Replication and transcription occur at

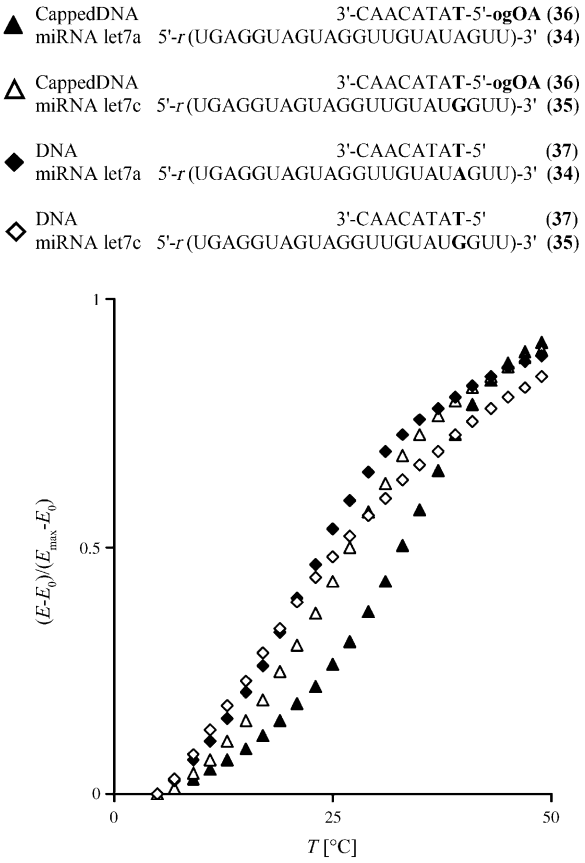

Figure 8. UV melting curves of duplexes between DNA octamer probes and two different microRNAs. The unmodified DNA probe (**37**) or the cap-bearing octamer probe **ogOA** (**36**) were allowed to bind to either of the targets. Only in the latter case was a significant melting point difference detected. Conditions: NaCl (1 M), sodium phosphate buffer (10 mM), DNA (1.5 μM), RNA (1.5 μM). Key: ▲ = **36**:**34**, △ = **36**:**35**, ◆ = **37**:**34**, ◇ = **37**:**35**.

the termini of base paired regions, and translation involves duplexes with two terminal and one internal base pair (codon:anticodon duplexes). Base pairing at the termini is also fascinating because it occurs in a conformationally less restricted molecular situation in which alternative base pairing arrangements are more readily realized and refolding or stacking of blunt ends is common. Therefore, studying base pairing at the termini is interesting not just for practical applications. Hybrid DNA:RNA duplexes are a species also formed during transcription and the formation of primers during replication. The fundamental interest in the molecular recognition at termini of DNA:RNA duplexes was one motivation for our current work that extends earlier work on DNA:DNA or RNA:RNA duplexes with modified dangling residues or caps.[45]

In the optimization phase of our study, we chose peptidic linkers (Scheme 1b) both for their flexibility, synthetic ease, and the modest lipophilicity of the chain. Some long chain alkanes can stabilize DNA:DNA duplexes,[46] but strongly lipophilic caps or linkers can lead to hydrophobic dimerization,[47] and can complicate purification due to strong adsorption or micelle formation. Many affinity-increasing terminal substituents known from the literature are fairly lipophilic.[34,48] From the results of our optimization it appears that a level of polarity that is typical for biologically active compounds, such as peptides and drugs, is well suited for increasing target affinity and base pairing selectivity, even in challenging cases such as purine–purine pairs at the terminus. The level of rigidity found for the optimized linker in **ogOA** seems to be a suitable compromise between flexibility (needed to adopt the proper binding conformation) and rigidity (needed to suppress too many alternative binding modes that would stabilize mismatched base pairs and to prevent too high an entropic cost for binding), at least within the limited structure space explored with our libraries.

It is also noteworthy that the optimized stacking moiety is the residue of a quinolone drug. Oxolinic acid is a gyrase inhibitor that is used clinically to combat bacterial infections and has found applications in fields as far from human health to fish farming.[49] Earlier combinatorial work from our laboratories, focused on other terminal base pairing arrangements, also identified quinolones as terminal acyl groups of caps.[22c,40] However, high resolution structures then revealed that the quinolones disrupted weak base pairs, rather than stabilizing them, a binding mode readily rationalized in the context of their activity as enzyme inhibitors, but not the desired mode of binding as a cap.[22c] Only when the terminal nucleoside residue was treated as a linker did a "composite cap" emerge that does indeed increase affinity and base pairing selectivity. In our study, we included a library member that features a nucleosidic linker, but the resulting conjugate was less successful as a high-affinity binder than other library members. Nevertheless, optimized cap **ogOA** does feature a phosphodiester linker, a five-membered ring, and amide linkages, much like the composite T*OA cap identified for DNA:DNA duplexes, in which T* stands for a 5′-amino-5′-deoxythymidine residue with an amide link to oxolinic acid (OA).[40]

Our results emphasize the importance of the linker. Although the strong propensity of quinolones to stack on nucleobases appears to be a driving force, unless the linker allows it to do so without disrupting weak base pairs (and contributes some binding affinity itself), no increase in sequence selectivity is imposed upon hybridization probes. What our study shows more than any previous work is that not just the length and lipophilicity of the linker is of importance, but also the conformational rigidity. Only when a ring structure (prolinol) was introduced, did the **OA**-terminated cap increase selectivity at the terminus for the difficult cases. More rigid structures (prolinol–proline) or the branched structures tested did not have the same favorable effect. This suggests to us that the **ogOA** cap constitutes at least a local optimum in structure space, in which linker and stacking moiety both interact favorably with the terminus of correctly paired strands in DNA:RNA duplexes. The new cap may aid the detection of biomedically relevant RNA sequences.

Experimental Section

General: Extinction coefficients of the modified oligonucleotides were calculated as the sum of the extinction coefficients of the unmodified DNA portion and the extinction coefficient of the stacking moieties at 260 nm given in the literature.[40]

UV melting experiments: Melting curve experiments used sodium phosphate buffer (10 mM) at pH 7 with NaCl concentrations of 150 mM or 1 M and strand concentrations of 1.0 μM for duplexes of **1** and **2** or 1.5 μM (each strand) for duplexes of **15**–**18**. For each sample, at least four curves from 5 to 80 °C were measured at a heating or cooling rate of 1 °C min^{-1}. Melting points were calculated using Templab 2.0, and the values given are the average of four curves. The hyperchromicity was calculated as the difference between the absorption at 80 °C and that at 5 °C, divided by the absorption at 5 °C.

Thermodynamic data: Thermodynamic data was determined by using Meltwin, version 3.5 through curve fitting, as described in reference [26]. For each duplex, four melting curves of 38 points were run. The values given are the average of four results ±1 standard deviation.

DNA synthesis: DNA oligonucleotides were synthesized on a 1 μmol scale, following a standard protocol of the manufacturer. Caps were introduced following the general protocols given below, after DMT deprotection of the DNA strands on controlled pore glass (cpg). General protocol A was used for the coupling of phosphoramidite-linker building blocks to the 5′-terminus of the DNA, followed by Fmoc deprotection[21] with piperidine in DMF (20 %) for 20 min, or MMT deprotection[17] with TCA deblock solution for DNA synthesis, depending on the linker building block. After deprotection of the terminal amino group of the linker, general protocol B was used for peptide coupling of Fmoc-protected amino acids or carboxylic acids. The oligonucleotides were deprotected and cleaved off the solid support by treatment with aqueous ammonia (1 mL, 25 %) at 55 °C for 2 h for oligonucleodides with an all-A/T sequence, and for 5 h for oligonucleotides with mixed sequences.[21] The ammonia was removed by blowing a low stream of nitrogen onto the surface of the solution for 1 h, followed by lyophilization.

Coupling of linker phosphoramidites to DNA (general protocol A): This protocol is similar to that reported earlier for manual chain extension of DNA.[17,23] Linker phosphoramidites (**5a**–**e**, **8**–**14**, **23**, and **28**–**30**, ca. 1 mg, 2 μmol, 60 equiv) were dried together with the DNA-bearing cpg (5 mg, ca. 0.16 μmol loading) for 2–20 h at 0.1 mbar. After addition of activator solution (0.25 M 4,5-dicyanoimidazol in CH_3CN, 40 μL) under argon, the mixture was agitated at 240 rpm on a vortexer for 2 h. Oxidizer solution for DNA synthesis (0.02 M I_2 in pyridine, THF, and water, 100 μL) was then added, and the mixture was again shaken for 15 min. The supernatant was removed, and the cpg was washed five times with acetonitrile (0.5 mL). Analytical samples were deprotected and cleaved from the cpg and evaluated by MALDI-TOF MS.

Peptide coupling on cpg (general protocol B): This procedure is similar to earlier protocols.[19d] The DNA-bearing cpg with strands with a terminal free amino group (**6a**–**f**, **6t**, **7b**–**d**, **24**–**27**; 5–7 mg, ca. 0.16 μmol DNA) were dried in a reaction vessel. The carboxylic acid (10 μmol) and HBTU (3 mg, 8 μmol) in DMF (100 μL) were treated with DIEA (4 μL, 31 μmol). After 5–20 min, the mixture was transferred to the cpg, followed by shaking for 15 min. In cases of low solubility of the carboxylic acid, the mixture was heated to 55 °C during the activation until a clear solution formed. After 20 min, the supernatant was removed and the cpg was washed twice with DMF (0.5 mL) and acetonitrile (0.5 mL).

HPLC purification: Modified oligonucleotides were purified by HPLC on a 250 mm × 4.6 mm 120–5 Nucleosil C4 or C18 column (Macherey–Nagel, Düren, Germany) with a gradient of CH_3CN in triethylammonium acetate buffer (TEAA; 0.1 M, pH 7). Yields are based on the amount of isolated pure product, compared to the loading of the cpg. Pure fractions were lyophilized, taken up in water, and lyophilized again.

***O*-2-Cyanoethyl-*O*-[*N*-fluorenylmethylcarboxyl)-(*S*)-pyrrolidin-3-methoxy](diisopropylamino)phosphoramidite (23)**: (*S*)-1-Fmoc-2-pyrrolidinemethanol (100 mg, 0.3 mmol) was dried and dissolved in CH_2Cl_2 (2 mL). After addition of DIEA (0.2 mL, 0.6 mmol), 2-cyanoethyl-*N*,*N*-diisopropylchlorophosphoramidite (140 μL, 0.6 mmol) was added dropwise at 0 °C, and the solution was stirred under argon. The ice bath was removed after 10 min and the solution was allowed to warm to room temperature, followed by stirring for 2.5 h. The mixture was diluted with CH_2Cl_2 (5 mL), and washed twice with saturated $NaHCO_3$ solution (5 mL) and brine (5 mL). The organic layer was dried over $MgSO_4$, and CH_2Cl_2 was removed in vacuo. The residue was purified by flash chromatography (silica, pretreated with eluent containing 2 % triethylamine, petroleum ether/ethyl acetate, 2:1, R_f = 0.85) to give **23** as a slightly yellow solid (126 mg, 0.24 mmol, 81 %). ^{31}P NMR (121 MHz, CD_3CN): δ = 147.7 ppm; ^{1}H NMR (300 MHz, CD_3CN): δ = 1.15 (dd, J = 10.5 Hz, J = 15.8 Hz, 12H), 1.85–1.97 (m, 6H), 3.35–3.82 (m, 6H), 4.18–4.48 (m, 2H), 7.29–7.86 ppm (m, 8H); MS (ESI): m/z calcd for $C_{29}H_{38}N_3O_4P$: 546.25 $[M+Na]^+$; found: 546.25.

Analytical data for HPLC-purified modified oligonucleotides and the MALDI-TOF mass spectra of these compounds are given in the Supporting Information.

Acknowledgements

The authors thank Dr. Amritraj Patra and Dr. Michael Printz for sharing melting curve data used for thermodynamic analyses, Denis Kusevic, Johanna Spörl and Ruth Frank for help with the synthesis of the linker building blocks, Sebastian Spies for providing oligonucleotides **1bCD**, **1bFL**, **1bCT**, **1bIA**, **1bPT**, **1bPA**, **1bAT**, **1bNP**, **1bPY**, and **1bPQ**, Dr. Eric Kervio for suggesting the use of 2′-fluoro-2′-deoxyuridine, and Helmut Griesser, Andreas Kaiser, Cora Prestinari, and Heike Vogel for a review of the manuscript. This work was supported by DFG (grant No. RI 1063/9–1) and the MINT program of the Ministry for Science Research and the Arts Baden-Württemberg (MWK) and febit holding GmbH (Heidelberg, Germany).

[1] M. Egli, W. Saenger, *Principles of Nucleic Acid Structure*, Springer, New York, **1984**.
[2] a) J. Knight, *Nature* **2003**, *425*, 232–233; b) W. C. Winkler, A. Nahvi, J. A. Collins, R. R. Breaker, *Nature* **2004**, *428*, 281–286; c) R. Micura, *Angew. Chem.* **2004**, *116*, 4797–4799; *Angew. Chem. Int. Ed.* **2004**, *43*, 4692–4694; d) R. T. Batey, S. D. Gilbert, R. K. Montange, *Nature* **2004**, *432*, 411–415; e) S. Thore, M. Leibundgut, N. Ban, *Science* **2006**, *312*, 1208–1211; f) D. G. Sashital, S. E. Butcher, *ACS Chem. Biol.* **2006**, *1*, 341–345.
[3] a) S. M. Elbashir, J. Harborth, W. Lendeckel, A. Yalcin, K. Weber, T. Tuschl, *Nature* **2001**, *411*, 494–498; b) G. Meister, T. Tuschl, *Nature* **2004**, *431*, 343–349.
[4] a) R. W. Carthew, *Science* **2006**, *313*, 305–306; b) N. C. Lau, A. G. Seto, J. Kim, S. Kuramochi-Miyagawa, T. Nakano, D. P. Bartel, R. E. Kingston, *Science* **2006**, *313*, 363–367.
[5] V. Ambros, B. Bartel, D. P. Bartel, C. B. Burge, J. C. Carrington, X. Chen, G. Dreyfuss, S. R. Eddy, S. Griffiths-Jones, M. Marshall, M. Matzke, G. Ruvkun, T. Tuschl, *RNA* **2003**, *9*, 277–279.
[6] S. Ambs, R. L. Prueitt, M. Yi, R. S. Hudson, T. M. Howe, F. Petrocca, T. A. Wallace, C. G. Liu, S. Volinia, G. A. Calin, H. G. Yfantis, R. M. Stephens, C. M. Croce, *Cancer Res.* **2008**, *68*, 6162–6170.
[7] For recent reviews, see: a) A. W. Wark, H. J. Lee, R. M. Corn, *Angew. Chem.* **2008**, *120*, 654–663; *Angew. Chem. Int. Ed.* **2008**, *47*, 644–652; b) B. Zhang, X. Pan, G. P. Cobb, T. A. Anderson, *Dev. Biol.* **2007**, *302*, 1–12; c) T. D. Schmittgen, E. J. Lee, J. Jiang, A. Sarkar, L. Yang L, T. S. Elton, C. Chen, *Methods* **2008**, *44*, 31–38.
[8] S. Fang, H. J. Lee, A. W. Wark, R. M. Corn, *J. Am. Chem. Soc.* **2006**, *128*, 14044–14046.
[9] B. Vester, J. Wengel, *Biochemistry* **2004**, *43*, 13233–13241.
[10] P. E. Nielsen, *Curr. Pharm. Des.* **2010**, *16*, 3118–3123.
[11] S. M. Gryaznov, *Chem. Biodiversity* **2010**, *7*, 477–493.
[12] a) S. Schmidt, A. Niemann, N. F. Krynetskaya, T. S. Oretskaya, V. G. Metelev, V. V. Sukhomlinov, Z. A. Shabarova, D. Cech, *Biochim.*

Biophys. Acta **1992**, *1130*, 41–46; b) T. Ono, M. Scalf, L. M. Smith, *Nucleic Acids Res.* **1997**, *25*, 4581–4588; c) A. Sabahi, J. Guidry, G. B. Inamati, M. Manoharan, P. Wittung-Stafshede, *Nucleic Acids Res.* **2001**, *29*, 2163–2170.

[13] a) R. W. Wagner, M. D. Matteucci, J. G. Lewis, A. J. Gutierrez, C. Moulds, B. C. Froehler, *Science* **1993**, *260*, 1510–1513; b) K.-Y. Lin, M. D. Matteucci, *J. Am. Chem. Soc.* **1998**, *120*, 8531–8532; c) J. A. Fidanza, G. H. McGall, *Nucleosides Nucleotides* **1999**, *18*, 1293–1295; d) H.-K. Nguyen, O. Fournier, U. Asseline, D. Dupret, N. T. Thuong, *Nucleic Acids Res.* **1999**, *27*, 1492–1498.

[14] T. Kottysch, C. Ahlborn, F. Brotzel, C. Richert, *Chem. Eur. J.* **2004**, *10*, 4017–4028.

[15] For selected references, see: a) R. L. Letsinger, G. G. Zhang, D. K. Sun, T. Ikeuchi, P. S. Sarin, *Proc. Natl. Acad. Sci. USA* **1989**, *86*, 6553–6556; b) N. T. Thuong, U. Asseline in *Oligonucleotides and Analogues: A Practical Approach* (Ed.: F. Eckstein), IRL Press, Oxford, **1991**, pp. 283–308; c) M. Manoharan, K. L. Tivel, T. P. Condon, L. K. Andrade, I. Barber-Peoch, G. Inamati, S. Shah, V. Mohan, M. J. Graham, C. F. Bennett, S. T. Crooke, P. D. Cook, *Nucleosides Nucleotides* **1997**, *16*, 1129–1138; d) K. M. Guckian, B. A. Schweitzer, R. X. F. Ren, C. J. Sheils, P. L. Paris, D. C. Tahmassebi, E. T. Kool, *J. Am. Chem. Soc.* **1996**, *118*, 8182–8183; e) T. E. Saison-Behmoaras, I. Duroux, N. T. Thuong, U. Asseline, C. Helene, *Antisense Nucleic Acid Drug Dev.* **1997**, *7*, 361–368; f) R. L. Letsinger, S. Chaturvedi, *Bioconjugate Chem.* **1998**, *9*, 826–830; g) D. A. Sarracino, J. A. Steinberg, M. T. Vergo, G. F. Woodworth, C. N. Tetzlaff, C. Richert, *Bioorg. Med. Chem. Lett.* **1998**, *8*, 2511–2516; h) R. Lucas, I. Gomez-Pinto, A. Avi, J. J. Reina, R. Eritja, C. Gonzalez, J. C. Morales, *J. Am. Chem. Soc.* **2011**, *133*, 1909–1916.

[16] C. Richert, P. Grünefeld, *Synlett* **2007**, 1–18.

[17] C. Ahlborn, K. Siegmund, C. Richert, *J. Am. Chem. Soc.* **2007**, *129*, 15218–15232.

[18] K. Siegmund, C. Ahlborn, C. Richert, *Nucleosides Nucleotides Nucl. Acids* **2008**, *27*, 376–388.

[19] a) T. V. Maltseva, P. Agback, M. N. Repkova, A. G. Venyaminova, E. M. Ivanova, A. Sandström, V. F. Zarytova, J. Chattopadhyaya, *Nucleic Acids Res.* **1994**, *22*, 5590–5599; b) C. F. Bleczinski, C. Richert, *J. Am. Chem. Soc.* **1999**, *121*, 10889–10894; c) O. P. Kryatova, W. H. Connors, C. F. Bleczinski, A. A. Mokhir, C. Richert, *Org. Lett.* **2001**, *3*, 987–990; d) A. A. Mokhir, C. N. Tetzlaff, S. Herzberger, A. Mosbacher, C. Richert, *J. Comb. Chem.* **2001**, *3*, 374–386; e) Z. Dogan, R. Paulini, J. A. Rojas Stütz, S. Narayanan, C. Richert, *J. Am. Chem. Soc.* **2004**, *126*, 4762–4763.

[20] A. Patra, C. Richert, *J. Am. Chem. Soc.* **2009**, *131*, 12671–12681.

[21] S. Narayanan, J. Gall, C. Richert, *Nucleic Acids Res.* **2004**, *32*, 2901–2911.

[22] a) J. Tuma, C. Richert, *Biochemistry* **2003**, *42*, 8957–8965; b) J. Tuma, R. Paulini, J. A. Rojas Stütz, C. Richert, *Biochemistry* **2004**, *43*, 15680–15687; c) K. Siegmund, S. Maheshwary, S. Narayanan, W. Connors, M. Riedrich, M. Printz, C. Richert, *Nucleic Acids Res.* **2005**, *33*, 4838–4848.

[23] M. Printz, C. Richert, *Chem. Eur. J.* **2009**, *15*, 3390–3402.

[24] H. Urakawa, S. El Fantroussi, H. Smidt, J. C. Smoot, E. H. Tribou, J. J. Kelly, P. A. Noble, D. A. Stahl, *Appl. Environ. Microbiol.* **2003**, *69*, 2848–2856.

[25] J. A. McDowell, D. H. Turner, *Biochemistry* **1996**, *35*, 14077–14089.

[26] M. Petersheim, D. H. Turner, *Biochemistry* **1983**, *22*, 256–263.

[27] J. Isaksson, J. Chattopadhyaya, *Biochemistry* **2005**, *44*, 5390–5401.

[28] a) P. J. Romaniuk, D. W. Hughes, R. J. Gregoire, T. Neilson, R. A. Bell, *J. Am. Chem. Soc.* **1978**, *100*, 3971–3972; b) S. M. Freier, B. J. Burger, D. Alkema, T. Neilson, D. H. Turner, *Biochemistry* **1983**, *22*, 6198–6206; c) S. M. Freier, D. Alkema, A. Sinclair, T. Neilson, D. H. Turner, *Biochemistry* **1985**, *24*, 4533–4539; d) N. Sugimoto, R. Kierzek, D. H. Turner, *Biochemistry* **1987**, *26*, 4554–4558; e) A. Lane, S. R. Martin, S. Ebel, T. Brown, *Biochemistry* **1992**, *31*, 12087–12095; f) M. E. Burkard, R. Kierzek, D. H. Turner, *J. Mol. Biol.* **1999**, *290*, 967–982; g) K. Ziomek, E. Kierzek, E. Biala, R. Kierzek, *Biophys. Chem.* **2002**, *97*, 243–249; h) P. V. Riccelli, K. E. Mandell, A. S. Benight, *Nucleic Acids Res.* **2002**, *30*, 4088–4093; i) T. Ohmichi, S.-i. Nakano, D. Miyoshi, N. Sugimoto, *J. Am. Chem. Soc.* **2002**, *124*, 10367–10372; j) J. Isaksson, S. Acharya, J. Barman, P. Cheruku, J. Chattopadhyaya, *Biochemistry* **2004**, *43*, 15996–16010.

[29] S. Bommarito, N. Peyret, J. Santa Lucia, Jr., *Nucleic Acids Res.* **2000**, *28*, 1929–1934.

[30] A. N. Amborski, P. E. Johnson, *J. Biomol. NMR* **2008**, *40*, 183–188.

[31] J. D. Liu, L. Zhao, T. B. Xia, *Biochemistry* **2008**, *47*, 5962–5975.

[32] K. Clanton-Arrowood, J. McGurk, S. J. Schroeder, *Biochemistry* **2008**, *47*, 13418–13427.

[33] F. H. C. Crick, *J. Mol. Biol.* **1966**, *19*, 548–555.

[34] a) R. X. F. Ren, N. C. Chaudhuri, P. L. Paris, S. Rumney, E. T. Kool, *J. Am. Chem. Soc.* **1996**, *118*, 7671–7678; b) S. Hainke, S. Arndt, O. Seitz, *Org. Biomol. Chem.* **2005**, *3*, 4233–4238.

[35] M. Manoharan, A. Akinc, R. K. Pandey, J. Qin, P. Hadwiger, M. John, K. Mills, K. Charisse, M. A. Maier, L. Nechev, E. M. Greene, P. S. Pallan, E. Rozners, K. G. Rajeev, M. Egli, *Angew. Chem.* **2011**, *123*, 2332–2336; *Angew. Chem. Int. Ed.* **2011**, *50*, 2284–2288.

[36] B. A. Connolly, *Nucleic Acids Res.* **1987**, *15*, 3131–3139.

[37] J. S. Mann, Y. Shibata, T. Meehan, *Bioconjugate Chem.* **1992**, *3*, 554–558.

[38] S. Miller, L. E. Jones, K. Giovannitti, D. Piper, M. J. Serra, *Nucleic Acids Res.* **2008**, *36*, 5652–5659.

[39] P. Hedge, R. Qi, K. Abernathy, S. Gay, S. Dharap, R. Gaspard, J. E. Hughes, E. Snesrud, N. Lee, J. A. Quackenbush, *BioTechniques* **2000**, *29*, 548–562.

[40] J. Tuma, W. H. Connors, D. H. Stitelman, C. Richert, *J. Am. Chem. Soc.* **2002**, *124*, 4236–4246.

[41] G. Makara, G. M. Keserü, A. Kovács, *J. Chem. Soc. Perkin Trans. 2* **1994**, 591–594.

[42] P. Kollman in *Nucleic Acids: Structures, Properties, and Functions* (Eds.: V. A. Bloomfield, D. M. Crothers, I. Tinoco, Jr.), University Science Books, Sausalito, **2000**, p. 282.

[43] D. Leaman, P. Y. Chen, J. Fak, A. Yalcin, M. Pearce, U. Unnerstall, D. S. Marks, C. Sander, T. Tuschl, U. Gaul, *Cell* **2005**, *121*, 1097–1108.

[44] A. L. Abbott, E. Alvarez-Saavedra, E. A. Miska, N. C. Lau, D. P. Bartel, H. R. Horvitz, V. Ambros, *Dev. Cell* **2005**, *9*, 403–414.

[45] For selected references, see: a) T. Maltseva, A. Sandström, I. M. Ivanova, D. S. Sergeyev, V. F. Zarytova, J. Chattopadhyaya, *J. Biochem. Biophys. Methods* **1993**, 26, 173–236; b) T. Maltseva, V. F. Zarytova, J. Chattopadhyaya, *J. Biochem. Biophys. Methods* **1995**, *30*, 163–177; c) H. Rosemeyer, F. Seela, *J. Chem. Soc. Perkin Trans. 2* **2002**, 746–750; d) K. Ziomek, E. Kierzek, E. Biala, R. Kierzek, *Biophys. Chem.* **2002**, *97*, 233–241; e) S.-i. Nakano, Y. Uotani, S. Nakashima, Y. Anno, M. Fujii, N. Sugimoto, *J. Am. Chem. Soc.* **2003**, *125*, 8086–8087; f) K. Siegmund, P. Daublain, Q. Wang, A. Trifonov, T. Fiebig, F. D. Lewis, *J. Phys. Chem. B* **2009**, *113*, 16276–16284; g) S. Nakano, H. Oka, Y. Uotani, K. Uenishi, M. Fujii, N. Sugimoto, *Mol. BioSyst.* **2010**, *6*, 2023–2029.

[46] B. M. Laing, L. Barrow-Laing, M. Harrington, E. C. Long, D. E. Bergstrom, *Bioconjugate Chem.* **2010**, *21*, 1537–1544.

[47] M. Hariharan, Y. Zheng, H. Long, T. A. Zeidan, G. C. Schatz, J. Vura-Weis, M. R. Wasielewski, X. Zuo, D. M. Tiede, F. D. Lewis, *J. Am. Chem. Soc.* **2009**, *131*, 5920–5929.

[48] A. Fülöp, X. Peng, M. M. Greenberg, A. Mokhir, *Chem. Commun.* **2010**, *46*, 5659–5661.

[49] a) J. G. Heddle, F. M. Barnard, L. M. Wentzell, A. Maxwell, *Nucleosides Nucleotides Nucl. Acids* **2000**, *19*, 1249–1264; b) L. A. Mitscher, *Chem. Rev.* **2005**, *105*, 559–592.

Received: June 15, 2011
Published online: September 20, 2011

